

## High-energy electron cooling in a collider

This content has been downloaded from IOPscience. Please scroll down to see the full text.

2006 New J. Phys. 8 283

(<http://iopscience.iop.org/1367-2630/8/11/283>)

View [the table of contents for this issue](#), or go to the [journal homepage](#) for more

Download details:

IP Address: 129.57.74.207

This content was downloaded on 21/03/2015 at 21:11

Please note that [terms and conditions apply](#).

## High-energy electron cooling in a collider

A V Fedotov<sup>1,4</sup>, I Ben-Zvi<sup>1</sup>, D L Bruhwiler<sup>2</sup>, V N Litvinenko<sup>1</sup>  
and A O Sidorin

<sup>1</sup> Brookhaven National Laboratory, Upton, NY 11973, USA

<sup>2</sup> Tech-X Corp., Boulder, CO 80303, USA

<sup>3</sup> Joint Institute for Nuclear Research, Dubna 141980, Russia

E-mail: [fedotov@bnl.gov](mailto:fedotov@bnl.gov)

*New Journal of Physics* **8** (2006) 283

Received 15 June 2006

Published 28 November 2006

Online at <http://www.njp.org/>

doi:10.1088/1367-2630/8/11/283

**Abstract.** High-energy electron cooling can open new possibilities in particle physics by producing high-quality hadron beams in colliders, and is presently considered for several accelerator physics projects. However, it also presents many unique features and challenges. For example, an accurate estimate of the cooling times requires a detailed calculation of the cooling process, which takes place simultaneously with various diffusive mechanisms. This task becomes even more challenging when the cooling is performed directly at a collision energy which puts special demands on the description of the beam distribution function under cooling. To address these issues, a systematic study of the cooling dynamics is underway at Brookhaven National Laboratory. In this paper, we present various aspects of this research and summarize our findings.

<sup>4</sup> Author to whom any correspondence should be addressed.

**Contents**

<b>1. Introduction</b>	<b>2</b>
<b>2. Cooling of the beam</b>	<b>3</b>
2.1. Magnetized and non-magnetized cooling . . . . .	3
2.2. Friction force with zero magnetic field . . . . .	3
2.3. Friction force with finite magnetic field . . . . .	4
2.4. Comparison with experimental data. . . . .	7
<b>3. Heating of the beam</b>	<b>8</b>
3.1. General models . . . . .	8
3.2. Comparison with experiments. . . . .	8
3.3. IBS for ion beam distribution under electron cooling. . . . .	9
<b>4. Cooling performance</b>	<b>11</b>
4.1. Detailed evolution of beam distribution. . . . .	11
4.2. Various scenarios of cooling. . . . .	13
<b>5. Summary</b>	<b>14</b>
<b>Acknowledgments</b>	<b>14</b>
<b>References</b>	<b>14</b>

**1. Introduction**

Electron cooling is an extremely useful technique for obtaining high-quality ion beams of high-intensity and low momentum spread [1]. In this method, the phase-space density of an ion beam is increased by means of a dissipative force—the dynamical friction (or velocity drag) on individual ions undergoing Coulomb collisions with a lower temperature electron distribution.

The electron cooling method found a wide range of applications in low-energy proton and ion storage rings. Cooled ion beams enable experiments under conditions unavailable otherwise, including the generation and storage of rare nuclei and short-lived isotopes, high-precision measurement of lifetimes for radioactive nuclides and of isotope masses, as well as other numerous applications [2]–[4].

The first relativistic cooling with relativistic parameter  $\gamma = 9.5$  was demonstrated in 2005 at Fermilab (FNAL), with cooled antiprotons being transferred for the experiments in a collider [5]. The high-energy cooling project for a relativistic heavy ion collider (RHIC) at Brookhaven National Laboratory (BNL) is unique compared to other cooling systems [6]–[8]. It considers cooling at  $\gamma = 107$  directly in a collider, which puts additional requirements on the description of the ion distribution function under cooling. This will be the first cooling system to use bunched electron beams, which allows to perform various beam manipulations. However, since the cooling times at high energy are much longer compared to standard low-energy cooling, quantitative calculation of cooling times are required with an accurate description of the cooling process.

In this paper, we summarize our findings from detailed study of the friction force both for the magnetized and non-magnetized cooling approaches. We also performed systematic study of various available models for the intra-beam scattering (IBS) and report comparison of theoretical models with experimental data. An accurate study of the cooling process which

requires description of beam distribution under cooling is discussed. The simulations presented are done using the VORPAL [9, 10] and BETACOOOL [11] codes.

## 2. Cooling of the beam

### 2.1. Magnetized and non-magnetized cooling

The traditional electron cooling system employed at any low-energy cooler is based on electron beam generated with an electrostatic electron gun in DC operating mode, immersed in a longitudinal magnetic field. The magnetic field is used for the transport of an electron beam through the cooling section from the gun to the collector. The magnetic field value is determined by the condition of electron ‘magnetization’—radius of the electron cyclotron rotation in the transverse plane has to be much less than the beam radius. The presence of a strong longitudinal magnetic field changes the collision kinetics significantly. The magnetic field limits transverse motion of the electrons. In the limit of a very strong magnetic field, the transverse degree of freedom does not take part in the energy exchange, because collisions are adiabatically slow relative to the cyclotron oscillations. As a result, the efficiency of electron cooling is determined mainly by the longitudinal velocity spread of the electrons. Such type of cooling is typically referred to as a ‘magnetized cooling’. Magnetized cooling was found to be an extremely useful technique in obtaining high-brightness hadron beams with extremely low longitudinal momentum spread [2].

However, if the rms velocity spread within the electron beam is comparable to or smaller than the spread within the ion beam, and there is no requirement to achieve ultra-cold ions, the cooling can be done without the help of a strong external magnetic field. Such cooling is referred to as non-magnetized cooling, although weak external fields may be employed, for example, to ensure focusing and alignment of electron and ion beams. The first cooling system which is based on the ‘non-magnetized’ approach was successfully constructed at the FNAL Recycler ring. It has been in operation since July 2005. This system is also the cooler with the highest energy, by far, of the electrons (4.3 MeV) in operation [5].

Extensive studies of the magnetized cooling approach for the RHIC showed that such an approach is feasible [6, 7] and would provide required increase in the luminosity for the RHIC-II upgrade. However, since an approach based on the non-magnetized electron beam significantly simplifies the cooler design, the baseline was recently changed to the non-magnetized one.

Generation and acceleration of the electron bunch without longitudinal magnetic field allows us to reach a low value of the emittance for the electron beam in the cooling section. The cooling rate required for suppression of IBS induced emittance growth can be achieved with  $\sim 5$  nC electron bunches ( $3 \times 10^{10}$  electrons per bunch). For cooling of Au ions in the RHIC at a beam energy of  $100 \text{ GeV n}^{-1}$ , the kinetic energy of the electron beam has to be 54.3 MeV. An Energy Recovery Linac (ERL) [8] will be needed to provide the required current continuously with high efficiency.

### 2.2. Friction force with zero magnetic field

The first step towards accurate calculation of cooling times is to use an accurate description of the cooling force.

With no magnetic field, the friction force on an ion inside a uniform density electron plasma with velocity distribution function  $f(v_e)$  is given by [12, 13]:

$$\vec{F} = -\frac{4\pi n_e e^4 Z^2}{m} \int L \frac{\vec{V}_i - \vec{v}_e}{|\vec{V}_i - \vec{v}_e|^3} f(v_e) d^3 v_e, \quad (1)$$

where  $Z$  is the ion charge number,  $e$  is the electron charge,  $n_e$  is the electron density,  $m$  is the electron mass,  $V_i$  and  $v_e$  are the ion and electron velocity, and  $L$  is the Coulomb logarithm  $L = \ln(\rho_{\max}/\rho_{\min})$  where  $\rho_{\max}$  and  $\rho_{\min}$  are the maximum and minimum impact parameters, respectively. An anisotropic velocity distribution  $f(v_e)$  can be approximated by a Maxwellian distribution with different temperatures for the longitudinal and transverse degrees of freedom. Simple asymptotic expressions for a typical situation in low-energy coolers when the transverse rms velocity spread of electrons  $\Delta_{e,\perp}$  is much larger than the longitudinal one  $\Delta_{e,\parallel}$  (which happens due to the electrostatic acceleration) have been obtained [13].

For an arbitrary ratio of the transverse and longitudinal temperatures of the electron beam, the friction force in equation (1) needs to be evaluated numerically. Such a numerical integration was recently implemented in BETACOOOL code [11]. In our studies, we found that in some cases, the asymptotic formulas can over estimate the friction force significantly, even for relatively large anisotropy of the rms velocities in the electron distribution. Therefore, if accuracy in the force values is a concern, the integration over velocity distribution in equation (1) should be done numerically.

In general, the Coulomb logarithm depends on the relative velocity and thus should be kept under the integral. In the assumption that the logarithm can be taken out of the integral, the three-dimensional integral in equation (1) can be reduced to a one-dimensional integral, as was suggested by Binney [14]. Such representation significantly speeds up the calculation, and was also implemented in the BETACOOOL code. We find that the result based on Binney's formulation agrees within 10% with a more accurate evaluation of equation (1), for azimuthally symmetric distributions.

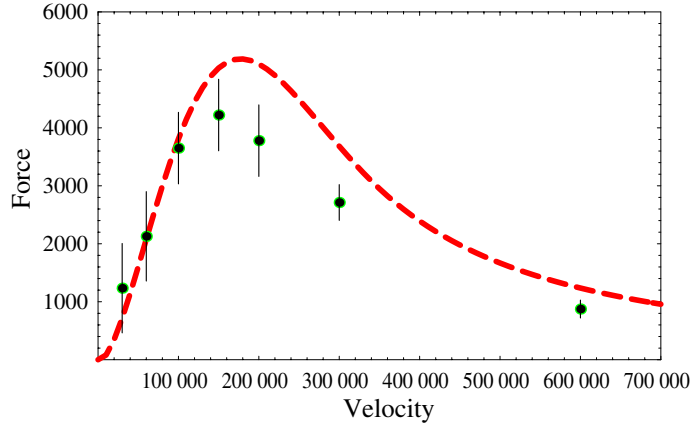
Numerical integration of equation (1) was further benchmarked with simulations using the VORPAL code [9, 10]. For simulation of electron cooling problem, VORPAL uses molecular dynamics techniques and explicitly resolves close binary collisions to obtain the friction force and diffusion coefficient with a minimum of physical assumptions [10].

Figure 1 compares VORPAL data (dots with error bars) with the results of numerical integration in equation (1) for the case of a Maxwellian distribution of electrons with rms velocity spreads of  $\Delta_{\parallel} = 1 \times 10^5$  and  $\Delta_{x,y} = 0.707 \times 10^5$  m s<sup>-1</sup> ( $Z = 79$ , and the density of electrons in the beam frame  $n_e = 2 \times 10^{15}$  m<sup>-3</sup>).

Simulations were done for various degrees of anisotropy of electron velocity as well. In general, we find agreement between VORPAL simulations and numeric integration in equation (1) within 10–15%, which we consider to be satisfactory.

### 2.3. Friction force with finite magnetic field

Description of Coulomb collisions in an external magnetic field is an interesting topic which found a lot of attention in both plasma and accelerator physics communities. The presence of a strong longitudinal magnetic field changes the collision kinetics, limiting the transverse motion of electrons. The combined effect of a strong magnetic field and strong velocity anisotropy of the electrons led to a well-known effect of 'fast magnetized cooling' [2].



**Figure 1.** Longitudinal component of the friction force ( $\text{eV m}^{-1}$ ) versus ion velocity ( $\text{m s}^{-1}$ ). Dashed line (red), numerical integration of equation (1); VORPAL results, dots with error bars.

A variety of theoretical models for the friction force have been developed (see, for example [4, 13, 15], and references therein). However, the available expressions make strong approximations, and the discrepancy between theory and experiments can be large.

In the presence of a finite-strength magnetic field, analytic treatments of the friction force have limitations. A practical expression reduced to a one-dimensional integral is possible only in the limit of a very strong magnetic field [13]. Such a result for the magnetized friction force was first obtained by Derbenev and Skrinsky [13]:

$$\vec{F} = -\frac{2\pi n_e e^4 Z^2}{m} \frac{\partial}{\partial \vec{V}} \int \left[ \frac{V_{\perp}^2}{U^3} L_M + \frac{2}{U} \right] f(v_e) dv_e, \quad (2)$$

where  $\vec{V} = (V_{\perp}, V_{\parallel})$  is the ion velocity, and  $U = \sqrt{V_{\perp}^2 + (V_{\parallel} - v_e)^2}$  is the relative velocity of the ion and an electron ‘cyclotron circle’, with transverse electron velocities assumed to be completely suppressed (i.e. approximation of infinite magnetic field). The actual values of the magnetic field and transverse rms electron velocity spread enter only via the cutoff parameters under the Coulomb logarithm, which is defined as  $L_M = \ln(\rho_{\max}/\rho_L)$ , where  $\rho_L = cm \Delta_{e,\perp}/(eB)$  is the radius of cyclotron rotation.

The function in equation (2) has asymptotes in the region of small ( $V \ll \Delta_{e,\parallel}$ ) and large ( $V \gg \Delta_{e,\parallel}$ ) ion velocities. These asymptotic expressions are useful qualitative guides, but are not sufficient for use in electron cooling system design, where accurate description of the friction force is needed for a large range of relative velocities between the ions and electrons.

The longitudinal force for the case of zero transverse ion velocity is plotted in figure 2. The VORPAL simulations presented are done for the following parameters: magnetic field in cooling solenoid  $B = 5 \text{ T}$ , time of interaction in the beam frame  $\tau = 0.4 \text{ ns}$ , the rms velocity spreads of the electron beam in the beam frame  $\Delta_{e,\perp} = 1.1 \times 10^7 \text{ m s}^{-1}$ ,  $\Delta_{e,\parallel} = 1.0 \times 10^5 \text{ m s}^{-1}$ ,  $Z = 79$  and the density of electrons in the beam frame  $n_e = 2 \times 10^{15} \text{ m}^{-3}$ .

One can see that the friction force expressions, which were constructed based on the asymptotic limits to cover a full range of relative velocities [4] can over estimate force values by a significant factor. The accuracy of the expression in equation (2) is itself of concern since it was

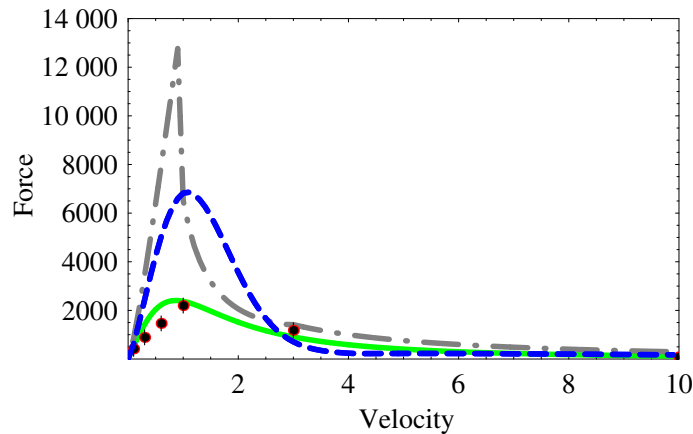


**Figure 2.** Longitudinal component of the force ( $\text{eV m}^{-1}$ ) versus velocity ( $\times 10^5 \text{ m s}^{-1}$ ). Asymptotic expressions [4], dot-dashed line (grey); equation (2) without the non-logarithmic term, dashed line (blue); empirical fit from [18], solid line (green); VORPAL results, dots with error bars.

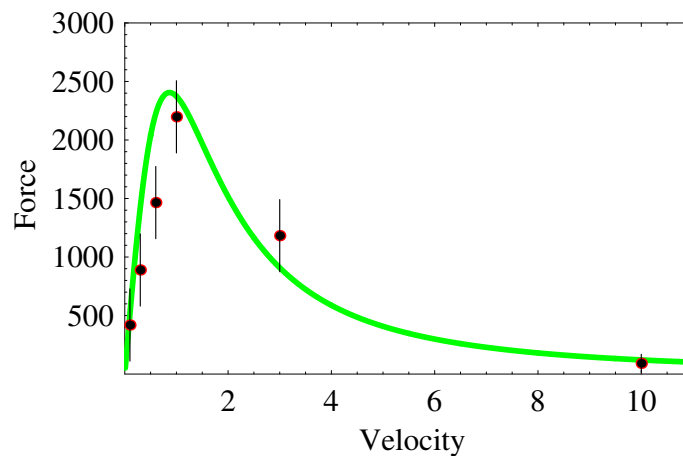


**Figure 3.** Longitudinal component of the force ( $\text{eV m}^{-1}$ ) versus velocity ( $\times 10^5 \text{ m s}^{-1}$ ) for zero transverse angle  $\theta = 0$  with respect to the magnetic field lines. VORPAL results, dots with error bars; empirical fit from [18], solid line.

obtained with several approximations, including an approximation of a very strong magnetic field. The limitations of this expression, especially at zero transverse angle were recently discussed in detail [16, 17].

For a practical situation with finite magnetic field, an empirical formula was introduced by Parkhomchuk in [18]. For the special case of zero transverse ion velocity, as in figure 2, we find that this empirical formula is in remarkable agreement with our simulation results using the VORPAL code. This is shown in figure 3, where the solid curve corresponds to empirical formula from [18] with the effective velocity spread equal to the longitudinal rms velocity spread of the electrons ( $\Delta_{e,\text{eff}} = \Delta_{e,\parallel}$ ) used in present simulations. The points with error bars are the VORPAL results. The observed agreement is reasonable, because this empirical formula was

obtained through systematic parametric fitting of longitudinal friction force measurements from experiments with ion beams that were already cooled and so had small transverse velocity spread.

Unfortunately, this empirical formula does not include the anisotropic behaviour of the friction force expected in the presence of a strong longitudinal magnetic field. For relative velocities larger than the longitudinal spread of the electrons, this model over estimates the friction force for some angles (with respect to the direction of the magnetic field lines), while underestimating it for others, compared to the VORPAL results [17]. However, direct numerical computation of the friction force shows only a weak dependence on angle. This was demonstrated by Parkhomchuk using simulations with zero-temperature electrons [18]. For finite temperature electrons, our simulations show even weaker dependence on angle [17]. These limitations of Parkhomchuk's empirical formula may average out to some extent, since for the net cooling power one needs to average over all particle amplitudes and phases.

As a result of our studies, we found that the use of equation (2) directly by means of numerical evaluation of the integral avoids significant over estimates of the friction force as compared to the asymptotic expressions. However, it requires the use of the non-logarithmic term (not necessarily justified in some cases) to prevent unphysical behaviour at high relative velocities. In addition, its functional behaviour at zero transverse ion velocity with the enhanced values for the force may be attributed to the limitation of the linearized dielectric approach to accurately treat close collisions. Thus, this expression should be used with caution [16].

For a simple estimate of the net cooling power and for finding basic parameters needed for an electron cooling system, use of the empirical expression from [18] seems sufficient. For an accurate description of the friction force in a magnetic field of arbitrary strength, with accuracy better than a factor of two, direct numerical simulations with a code like VORPAL are required.

#### 2.4. Comparison with experimental data

The friction force as a function of various parameters was extensively explored in many low-energy coolers (see, for example [4], [19]–[22], and references therein).

A series of dedicated measurements of the longitudinal magnetized friction force was recently performed at the circular ion accelerator CELSIUS [23], which includes an electron cooling section. The goal of the measurements was to obtain data suitable for a detailed quantitative comparison with theoretical models and simulations. The longitudinal friction force was measured using the phase-shift method with a bunched ion beam, which is based on measuring the phase difference between the RF system and the ion beam. High precision in the measurements was obtained through a combination of two techniques: (i) changing the RF frequency instead of the electron voltage, and (ii) accurate measurements of the phase difference using a phase discriminator.

The friction force was measured for various parameters of the cooler, including different electron beam currents, various magnetic field strengths, different strengths of the magnetic field errors in the cooling solenoid and the misalignment angle between the electron and ion beams. In addition, standard parameters of the cooler were altered in order to explore effects that are essential for the understanding of high-energy magnetized cooling, such as treatment of IBS for non-Gaussian distributions. Some comparison of these measurements with the theoretical models was also reported [24].

For the non-magnetized force, uncertainties in the theoretical friction force expressions are relatively small, but comparison with experiments is obscured by the dependence on the



transverse rms velocity spread within electron beam, which is no longer suppressed by the magnetic field, making its effect on the force value very strong. As a result, accurate interpretation of experimental data requires careful characterization of the electron beam, an effort which is presently being attempted at the FNAL cooler [5, 25].

Our numerical approach using the VORPAL code is capable of simulating experimental data obtained in low-energy coolers as well, although in some cases simulations become more complicated since they require inclusion of electron-electron interactions in addition to electron-ion interactions [17, 26].

For the case of non-magnetized cooling at FNAL, several new algorithms were implemented in BETACOOOL code which allow direct simulation of the procedures of the drag rate measurement used there, as well as simulation of the evolution of the antiproton beam distribution during such measurements [27]. Initial comparison of the experimental data with the simulations was recently reported [28].

### 3. Heating of the beam

The present performance of the RHIC collider with heavy ions is limited by IBS. Such a process is typically separated in two effects: (i) scattering on a large angle so that the particles can be lost from the bunch during a single collision, called the Touschek effect, and (ii) scattering on small angles which randomly add together and can increase the phase space volume of the beam, called IBS.

#### 3.1. General models

A theory of IBS for proton beams was proposed by Piwinski [29]. This model was later extended by a CERN team in collaboration with Piwinski to include variations of the lattice functions around the ring. An improved model was described in a detailed report by Martini [30]. Similar results were also obtained with a completely different approach of S-matrix formalism by Bjorken and Mtingwa [31].

For RHIC parameters at collision energy of  $100 \text{ GeV } n^{-1}$  (which is well above the transition energy), we found that the growth rates using both Martini's and Bjorken-Mtingwa's models were within a few percent agreement with one another. For our numerical studies of electron cooling presented in this report, Martini's model was used without any approximation. We also used an exact designed lattice of the RHIC which includes the derivatives of the lattice functions and insertions in the straight sections for the interaction points.

#### 3.2. Comparison with experiments

Since the main goal of electron cooling for the RHIC is to overcome emittance growth due to IBS, it was extremely important to make sure that the models of IBS which are being used in cooling simulations are in a good agreement with experimentally measured growth rates.

Several dedicated IBS experiments were performed in 2004 with Au and in 2005 with Cu ions to increase the accuracy and parameter range of previous IBS measurements [32]. For this purpose, bunches of various intensity and emittance were injected, and growth rates of both the horizontal and vertical emittance and the bunch length in each individual bunch were recorded

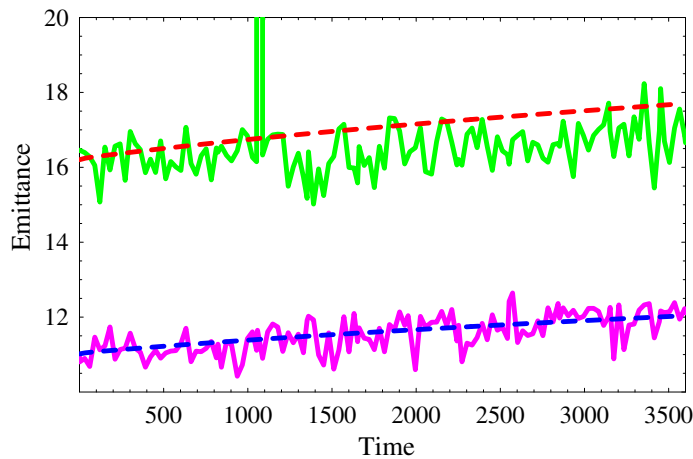


**Figure 4.** Horizontal and vertical 95% normalized emittance ( $\mu\text{m}$ ) versus time (seconds) for bunch intensity  $2.9 \times 10^9$  Cu ions. Measured emittance: top green curve (horizontal), bottom pink curve (vertical). BETACOOL simulation using Martini's model: top red dashed line (horizontal), blue dashed line (vertical).

with the Ionization Profile Monitor (IPM) and the Wall Current Monitor (WCM), respectively. Other effects which may obscure comparison, like beam-beam collisions, were turned off. Experiments were done with the RF harmonic  $h = 360$  allowing growth of the longitudinal profile without losses from the bucket.

The latest data for IBS with Cu ions showed very good agreement between the measurements and Martini's model of IBS for the exact RHIC lattice. Figure 4 shows comparison of simulations versus measurements for the growth of the horizontal and vertical emittance for a single bunch of Cu ions with intensity of  $2.9 \times 10^9$ . Analysis were performed for bunches with different intensity and initial emittance. The measured growth rate was found to scale with the bunch intensity and the value of the initial emittance as expected for the IBS growth rates for energies well above the transition energy. More details on comparison of experimental data with theory can be found in [33, 34].

Note, that conditions of the 'dedicated IBS experiments' (presented in this subsection) are different from a typical settings during RHIC operation with ions. Such conditions were specifically chosen to provide a clean comparison between the IBS theory and measurements. In reality, during a standard operation, one uses RF cavity with harmonic  $h = 2520$ . A resulting emittance growth in such a case is much stronger than the one shown in figure 4, and is similar to the one seen in figure 8.

### 3.3. IBS for ion beam distribution under electron cooling

Standard models of IBS discussed in subsection 3.2 are based on the growth rates of the rms beam parameters for the Gaussian distribution. In the absence of beam loss and without electron cooling, the time evolution of the beam profiles in the RHIC is approximated with a Gaussian distribution with a good accuracy.

However, when electron cooling is introduced, the beam distribution quickly deviates from Gaussian. An example of simulated distribution is shown in figure 5 for the parameters of the

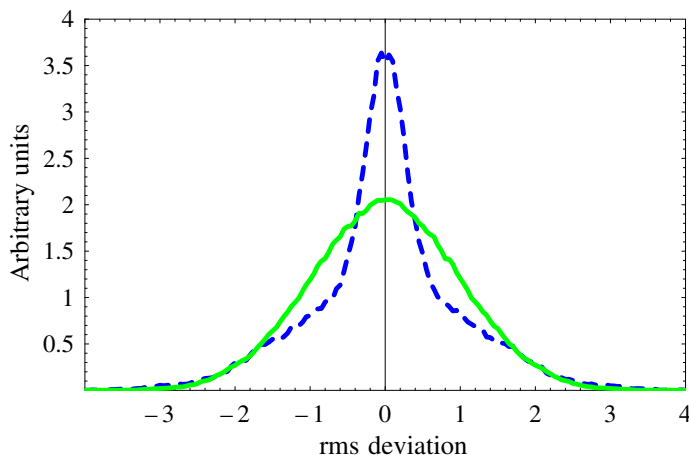


**Figure 5.** BETACOOOL simulation of the transverse profiles of the ion beam for the RHIC cooler parameters [7] based on the magnetized cooling approach. Solid (green) line, initial distribution; dashed (blue) line, distribution after 30 min of cooling.

magnetized cooling of the RHIC [7]. The formation of the non-Gaussian profiles during the cooling process were also experimentally recorded to provide the data for the verification of the IBS models for such distributions [24].

To address such a process, the IBS theory was recently reformulated for a bi-Gaussian distribution by Parzen [35]. A detailed analytic treatment of IBS, which depends on individual particle amplitude was proposed by Burov [36], with an analytic formulation done for a flattened Gaussian distribution (longitudinal rms velocity spread in beam frame is negligible compared to the transverse one). Also, a simplified ‘core-tail’ model, based on different diffusion coefficients for beam core and tails was proposed [37]. The above formulations, which attempt to calculate IBS for a beam distribution changing under electron cooling, were implemented in BETACOOOL code and were used for cooling studies of the RHIC. The major goal was to produce a reasonable estimate of the expected luminosity gain for such distributions.

A more accurate estimate of the luminosity gain requires further improvements of our IBS models for non-Gaussian distributions with an accurate description of the IBS not just for the core of the distribution but for the tails as well. This work is presently in progress with new treatments of IBS recently implemented in BETACOOOL, including the kinetic model [38] and local diffusion model [39]. An alternative approach of IBS treatment for an arbitrary distribution similar to the one used in MOCAC code [40] is also being considered.

In our studies, we found that the difference between various models and resulting integrated luminosity is substantial for the previous approach of the magnetized cooling where a formation of a distribution with a sharp core is observed [37], as shown in figure 5. One can see formation of a dense core after 30 min of cooling (at  $\gamma = 107$ ). Similar profiles are observed in standard low-energy coolers but on much shorter time scale of, typically, less than a second.

For the present parameters of electron cooling in the RHIC [41], which is based on the non-magnetized cooling approach, the formation of such a bi-Gaussian distribution is less pronounced than before for the case of the magnetized cooling. As a result, a deviation between various models and the difference in the integrated luminosity being predicted is expected to be less crucial. The

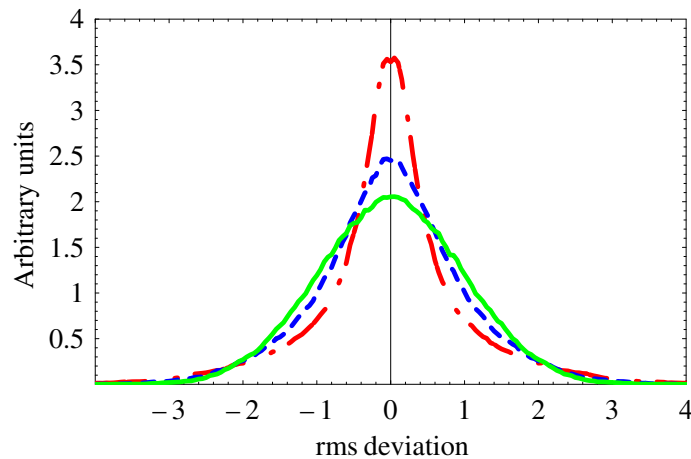


**Figure 6.** BETACOOOL simulation of the transverse profiles of the ion beam based on the non-magnetized cooling approach. Solid (green) line, initial distribution; dashed (blue) line, distribution after 30 min of cooling. Dot-dashed (red) curve, distribution after 2 h of cooling.

evolution of ion beam profiles for the present parameters of the non-magnetized cooling of the RHIC is shown in figure 6 which shows that distribution stays close to Gaussian even after two hours of cooling. More accurate algorithms for the IBS of such distributions are presently being developed to reduce remaining uncertainty.

## 4. Cooling performance

### 4.1. Detailed evolution of beam distribution

A quick estimate of the cooler performance can be done using an approach with a dynamical tracking of the rms beam parameters. For the previous design with magnetized cooling for the RHIC, when a detailed treatment of the beam distribution with a pronounced core was extremely important, we found that such an approach may be too inaccurate [37]. For the case of fast cooling in typical low-energy coolers where the whole Gaussian beam is quickly cooled to an approximately Gaussian distribution with much smaller rms parameters, a simple approach based on the rms dynamics provides reasonably accurate estimates. For the present parameters of the RHIC cooler based on the non-magnetized approach most of the particles with amplitudes within a few rms deviations are also effectively cooled, making an rms dynamics approach a reasonable estimate as well.

The luminosity performance for the RHIC-II upgrade with Au ions at  $100 \text{ GeV n}^{-1}$  beam energy is shown in figures 7 and 9, using BETACOOOL simulation [11] based on the rms and detailed beam approach, respectively. For simulations presented, we used the following parameters of RHIC cooler based on the non-magnetized approach: cooling section  $L = 80 \text{ m}$ , electron charge  $5 \text{ nC}$ , rms normalized emittance of electrons  $4 \mu\text{m}$ , rms momentum spread of electrons  $3 \times 10^{-4}$ , undulator (to suppress recombination [7]) with period  $8 \text{ cm}$  and magnetic field of  $10 \text{ G}$ . The parameters of the Au ion beam are the following:  $1 \times 10^9$  particles per bunch, 112 bunches, initial 95% normalized emittance  $15 \mu\text{m}$  initial rms momentum spread  $5 \times 10^{-4}$

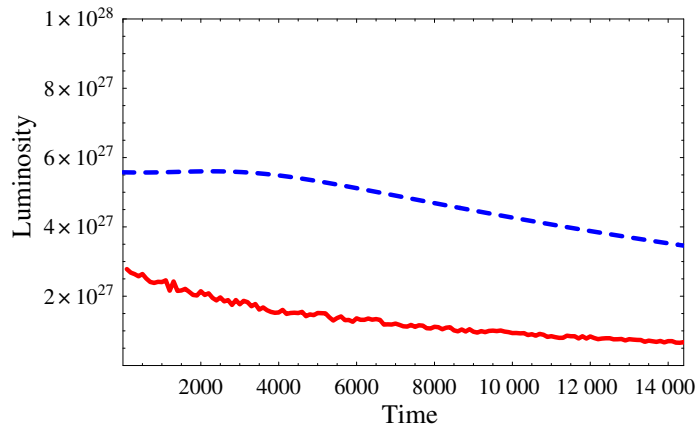


**Figure 7.** Luminosity ( $\text{cm}^2 \text{s}^{-1}$ ) versus time (seconds) based on the rms dynamics approach. Dashed (blue) line, luminosity for the RHIC-II for Au ions at  $100 \text{ GeV n}^{-1}$  with cooling; solid (red) line, luminosity for the RHIC-II for Au ions without cooling.

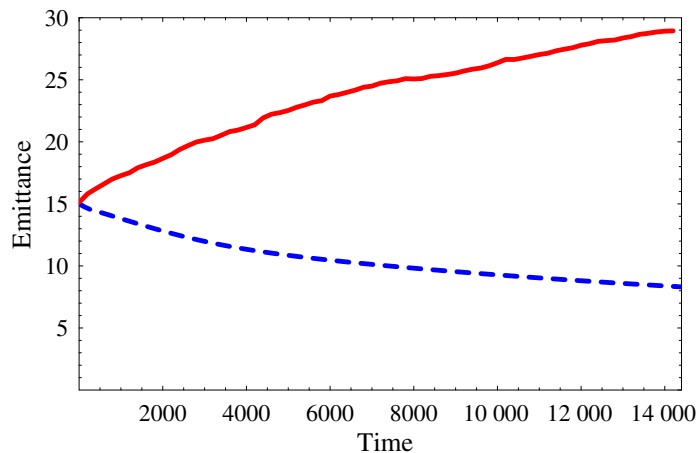


**Figure 8.** 95% normalized transverse emittance ( $\mu\text{m}$ ) versus time (seconds) for Au ions and parameters of the RHIC-II upgrade, corresponding to figure 7. BETACOOL simulations: solid (red) curve, emittance growth due to the IBS without cooling; dashed (blue) curve, emittance with cooling using rms dynamics approach.

and initial rms bunch length 18 cm. For the case without electron cooling we used beta function in interaction point  $\beta^* = 1 \text{ m}$ , while for the case with electron cooling we used  $\beta^* = 0.5 \text{ m}$ . The resulting average luminosity with cooling during 4 h store is  $\langle L \rangle = 5 \times 10^{27}$  and  $7 \times 10^{27} \text{ cm}^2 \text{ s}^{-1}$  for figures 7 and 9, respectively.

Note that for present parameters of electron cooler for the RHIC, the transverse rms emittance is cooled only slightly, as can be seen in figure 8 using the rms dynamics approach or from beam profiles in figure 6, which are obtained using a more accurate ‘detailed beam’ approach in BETACOOL simulations. Such modest cooling corresponds to a slight increase in

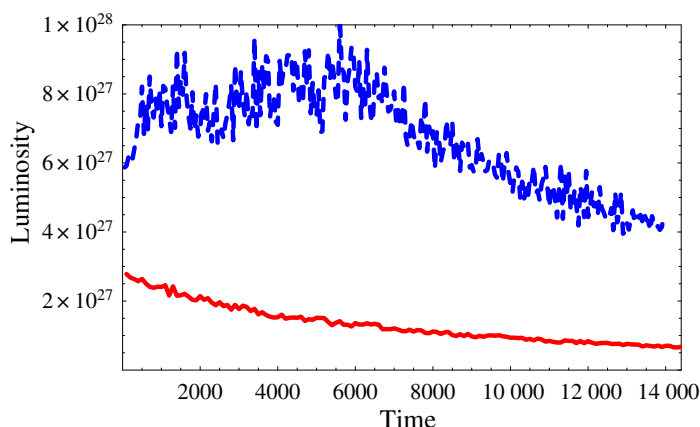


**Figure 9.** Luminosity ( $\text{cm}^2 \text{s}^{-1}$ ) versus time (seconds) based on the approach with detailed evolution of beam distribution. Dashed (blue) line, luminosity for the RHIC-II for Au ions at  $100 \text{ GeV n}^{-1}$  with cooling; solid (red) line, luminosity for the RHIC-II for Au ions without cooling.

peak luminosity in figure 9. The real difference in average luminosity per store between the case with and without cooling comes from the fact that without cooling emittance has a strong growth, shown in figure 8. Such a growth of emittance has major contribution to luminosity loss without cooling, shown in figure 9.

Also, as a result of such emittance growth, further significant reduction of the  $\beta^*$  below 1 m would lead to a significant angular spread and beam loss. On the other hand, keeping rms emittance approximately constant (by cooling), allows us to start a store cycle with smaller values of the  $\beta^*$  [7], which results in larger initial peak luminosity with cooling, as shown in figure 9.

Additional luminosity loss without cooling comes from the longitudinal IBS which results in particle loss from the bucket. Electron cooling prevents growth of both the transverse and longitudinal emittances. The drop in the luminosity observed in figure 9 for the case with electron cooling is due an effect of beam disintegration in collisions for such high luminosities. The cross section of such a ‘burn-off’ process (from dissociation and bound electron-positron pair production) for Au ions at  $100 \text{ GeV n}^{-1}$  is about 212 (barn) which limits the store time. Various manipulations with electron beam, such as dynamic change of beam radius and beam charge may help to maintain luminosity at constant level for a longer period of time. Such schemes are presently under development.

#### 4.2. Various scenarios of cooling

There are various possibilities of using electron cooling at the RHIC [6, 7]. Direct cooling at the top energy is considered as a base line approach for RHIC-II. However, for the eRHIC project [42], it is important that cooling is fast enough to allow reduction of the rms beam parameters, especially the rms bunch length. In this case, pre-cooling at low energy becomes very attractive due to a very strong dependence of the cooling time on energy. For the same reason, cooling is very effective for scenarios with collisions at low energy.

Electron cooling of Au ions at storage energy of  $100 \text{ GeV n}^{-1}$  allows to reach desired increase in the integrated average luminosity for the RHIC-II upgrade, which is a factor of 40 increase compared to designed RHIC values. The longitudinal cooling which prevents bunch length from

growing, also maximizes the useful interaction region, increasing an effective luminosity in the detector.

For Au–Au collisions at  $100 \text{ GeV n}^{-1}$  with electron cooling, the store time is limited to about 4 h due to a rapid ‘burn-off’ in the IP. However, for other ions species, for which the cross section of such a process is small, longer stores can be tolerated with essentially constant luminosity.

## 5. Summary

Motivated by the design of the high-energy cooling system for the RHIC, a detailed study of the cooling process is being performed at the Brookhaven National Laboratory. The goal of this study is to provide an accurate description of the friction force both with and without external magnetic field in the cooler. Many new aspects of the cooling dynamics needed for accurate description of the cooling process in a collider mode were revealed as a result of detailed treatment of the ion distribution function under cooling. The study performed allows us to have a reliable design of the high-energy cooling system.

## Acknowledgments

We are indebted to the Accelerator Physics group of the RHIC Electron Cooling Project for constant support and many useful suggestions. We thank A Burov, Ya Derbenev, D Kayran and G Parzen for many useful discussions of related topics. Comparison of IBS models with the measurements in the RHIC is a result of help by W Fischer, S Tepikian and J Wei, which is greatly appreciated. We are grateful to the Tech-X Corp. team (Colorado, USA) and the Dubna cooling group (JINR, Russia) for the support and help with the VORPAL and BETACOOOL codes, respectively. This work is supported by the US DOE Office of Science, Office of Nuclear Physics. DLB was supported by grant no. DE-FG02-04ER84094.

## References

- [1] Budker G I 1967 *At. Energ.* **22** 346
- [2] Parkhomchuk V V and Skrinsky A N 1991 *Rep. Prog. Phys.* **54** 919
- [3] Larsson M 1995 *Rep. Prog. Phys.* **58** 1267
- [4] Meshkov I 1997 *Nucl. Instrum. Methods A* **391** 1
- [5] Nagaitsev S *et al* 2006 *Phys. Rev. Lett.* **96** 044801
- [6] Parkhomchuk V V and Ben-Zvi I 2001 *BNL Tech. Rep.* C-AD/AP/47
- [7] Fedotov A V, Ben-Zvi I, Litvinenko V N, Sidorin A, Smirnov A and Trubnikov G 2005 *Proc. Conf. 2005 Particle Accelerator (Knoxville, TN)* p 4236
- [8] Ben-Zvi I 2006 *AIP Conf. Proc.* **821** 75
- [9] Nieter C and Cary J 2004 *J. Comp. Phys.* **196** 448
- [10] Bruhwiler D L *et al* 2005 *AIP Conf. Proc.* **773** 394
- [11] Sidorin A O, Meshkov I N, Seleznev I A, Smirnov A V, Syresin E M and Trubnikov G V 2006 *Nucl. Instrum. Methods A* **558** 325
- [12] Chandrasekhar S 1942 *Principles of Stellar Dynamics* (Chicago: University of Chicago Press)
- [13] Derbenev Ya S and Skrinsky A N 1978 *Part. Acc.* **8** 235
- [14] Binney J J 1977 *Mon. Not. R. Astron. Soc.* **181** 735
- [15] Sorensen A H and Bonderup E 1983 *Nucl. Instrum. Methods* **215** 27

- [16] Fedotov A V, Bruhwiler D L and Sidorin A O 2006 *Proc. 39th ICFA Advanced Beam Dynamics Workshop HB2006 (KEK, Tsukuba, Japan)*
- [17] Fedotov A V, Bruhwiler D L, Sidorin A O, Abell D T, Ben-Zvi I, Busby R, Cary J R and Litvinenko V N 2006 *Phys. Rev. ST Accel. Beams* **9** 074401
- [18] Parkhomchuk V V 2000 *Nucl. Instrum. Methods A* **441** 9
- [19] Danared H 1997 *Nucl. Instrum. Methods A* **391** 24
- [20] Dikansky N S, Kudelainen V I, Lebedev V A, Meshkov I N, Parkhomchuk V V, Sery A A, Skrinsky A N and Sukhina B N 1988 *BNP Tech. Report* 88-61 (Novosibirsk, Russia: Institute of Nuclear Physics)
- [21] Winkler T, Beckert K, Bosch F, Eickhoff H, Franzke B, Nolden F, Reich H, Schlitt B and Steck M 1997 *Nucl. Instrum. Methods A* **391** 12
- [22] Beutelspacher M, Fadil H, Furukawa T, Grieser M, Noda A, Noda K, Schwalm D, Shirai T and Wolf A 2003 *Nucl. Instrum. Methods A* **552** 123
- [23] Ekstrom C *et al* 1988 *Phys. Scr. T* **22** 256–68
- [24] Fedotov A V, Gálnander B, Litvinenko V N, Lofnes T, Sidorin A, Smirnov A and Ziemann V 2006 *Phys. Rev. E* **73** 066503
- [25] Prost L *et al* 2006 *Proc. 39th ICFA Advanced Beam Dynamics Workshop HB2006 (KEK, Tsukuba, Japan)*
- [26] Bruhwiler D L, Busby R, Abell D T, Veitzer S, Fedotov A V and Litvinenko V N 2005 *Proc. Conf. 2005 Particle Accelerator (Knoxville, TN)* p 4206
- [27] Sidorin A and Smirnov A 2005 *BNL Report on BETACOOOL Development* <http://www.bnl.gov/cad/ecooling>
- [28] Fedotov A V 2006 Presentation *RHIC Electron Cooling Workshop (Upton, NY, May)* online at <http://www.bnl.gov/cad/ecooling/>
- [29] Piwinski A 1974 *Proc. 9th Int. Conf. High Energy Acc. (SLAC, Stanford)* p 405  
Piwinski A 1992 *CERN Report* 92-01 p 226
- [30] Martini M 1984 *CERN Report* PS/84-9 (AA)
- [31] Bjorken J and Mtingwa S 1983 *Part. Accl.* **13** 115
- [32] Fischer W *et al* 2002 *European Particle Accelerator Conf. (Paris, France)* p 236
- [33] Wei J, Fedotov A, Fischer W, Malitsky N, Parzen G and Qiang J 2005 *AIP Conf. Proc.* **773** 389
- [34] Fedotov A V, Fischer W, Tepikian S and Wei J 2006 *Proc. 39th ICFA Advanced Beam Dynamics Workshop HB2006 (KEK, Tsukuba, Japan)*
- [35] Parzen G 2004 *BNL Tech. Notes* C-AD/AP/144, C-AD/AP/150
- [36] Burov A 2003 *FNAL Tech. Note* FNL-TM-2258
- [37] Fedotov A V *et al* 2005 *Proc. Conf. 2005 Particle Accelerator (Knoxville, TN)* p 4263
- [38] Zenkevich P, Boine-Frankenheim O and Bolshakov A 2006 *Nucl. Instrum. Methods A* **561** 284
- [39] Sidorin A 2006 Presentation *RHIC Electron Cooling Workshop (Upton, NY)* online at <http://www.bnl.gov/cad/ecooling/>
- [40] Alexeev N N *et al* 1998 *AIP Conf. Proc.* **480** 31  
Zenkevich P R *et al* 2001 *Proc. COOL01 Workshop (Bad Honnef)*
- [41] RHIC electron cooling, online at <http://www.bnl.gov/cad/ecooling>
- [42] Ptitsyn V *et al* 2004 *eRHIC Proc. Conf. 2004 European Particle Accelerator (Lucerne, Switzerland)* p 923